Experimental Analysis of Immersion & Invariance Adaptive Control for an Interleaved DC/DC Boost Converter with Unknown Load Type

Jan Wachter, Lutz Gröll and Veit Hagenmeyer
Karlsruhe Institute of Technology, Institute for Automation and Applied Informatics, Karlsruhe, Germany
jan.wachter@kit.edu

***Abstract*—The retrofit of the energy system leads to new challenges for the control of power electronic devices. To account for parametric uncertainties of passive elements, or unknown ambient conditions in real-world applications, the use of proportional-integral (PI) controllers in cascaded schemes is common. Observer based adaptive control approaches can be leveraged to accommodate such uncertainties and at the same time provide parameter estimates and enable model based control approaches. From an application perspective, the question arises about the consequences of wrong modelling assumptions, for example regarding the often unknown load type. In this work an interleaved DC/DC boost converter is considered, that supplies a DC-bus to which generally unknown loads can be connected, such as a grid-tied three phase inverter. This paper illustrates the design of an observer based adaptive controller using the Immersion & Invariance framework with an energy shaping plus damping injection passivity based controller. A highly simplified, large signal plant model as well as the assumption of a purely resistive load are used for the design. The provided experimental results show that the adaptive controller is able to cope with violations of the modeling assumptions concerning the load type in a real-world application scenario.**

***Index Terms*—adpative control, interleaved dc/dc boost converter, power electronics, modelling assumption violation**

I. Introduction

The transition of the power grid towards carbon neutral technologies causes a fast rising number of power electronically interfaced distributed generation devices. This has inherent new challenges for ensuring compliant behavior of power electronic devices in the face of uncertain ambient conditions [1]. For real-world applications the concept of cascaded control systems is widely used for a large variety of converter types since it is easily expandable. For example, an inner current control loop can be expanded by an outer voltage control loop in case of a grid forming device or a power control loop for grid feeding applications [2]. To accommodate uncertainties in the plant and changing ambient conditions, these concepts often rely on proportional-integral (PI) controllers due to their robustness and existing experience from many engineering applications. By this, the desired control objective is achieved, but the information about the changed conditions or parameters is not accessible. However, extracting such information is of special interest since it can be used in cyber-security applications such as false data injection detection or simply to reduce system costs by omitting sensors while maintaining plug-and-play abilities. Observer based adaptive controllers are well suited for such settings: fulfilling the control objective under uncertainty while providing parameter estimates.

For this, a well suited approach is the Immersion & Invariance (I&I) framework [3], since it allows for a modular design of the controller and the observer based adaptation. This approach has been successfully applied for an input voltage and resistive load observer of a DC/DC boost converter in [4], and extended to an adaptive output-feedback scheme in [5]. Further, the design of I&I based adaptive controllers for DC/DC buck, boost and buck-boost converters connected to constant power loads (CPL) is presented in [6]–[9]. An I&I observer application for fault analysis of power electronic components is presented by [10].

The aforementioned contributions show results for setups that comply with the modelling assumptions. However, this can not be ensured for practical plug-and-play scenarios. For example the load type, e.g. resistive, constant current or power, is not known or might even change as in the presented experiments. The present work is concerned with the following questions that arise from an application point of view: which level of detail for the model is required and how sensitive is the approach to the violation of modelling assumptions. Towards this, the present paper provides the following contributions

1) The design of an observer based I&I adaptive controller for an interleaved DC/DC boost converter is illustrated based on a highly simplified model and restrictive assumptions for the load type. Further the controller is implemented on prototyping hardware.
2) The consequences of modelling assumption violations are experimentally analysed. For this, several scenarios are considered, e.g. non-resistive load, changes of the load type, sudden changes of the unmeasured supply voltage, which violate the assumptions made during design. The results show that the approach is able to cope with those violations in terms of output regulation as well as providing parameter estimates.

The remainder of this paper is organized as following, Section II presents the system under study and the modelling assumptions. In Section III, the adaptive control design is detailed. Section IV presents and discusses the experimental setup and

979-8-3503-9678-2/23/.00

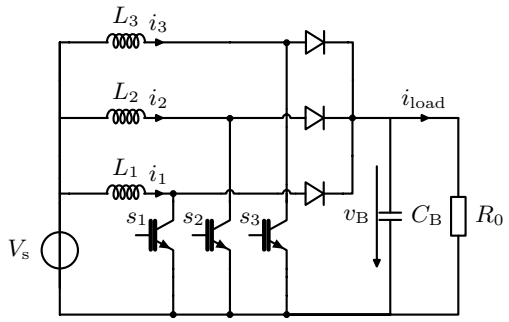

Fig. 1. Simplified circuit diagram with applied load model

results. Lastly, Section V concludes the paper.

II. System under Study

In the following, we consider an interleaved DC/DC boost converter with three legs that supplies a DC-bus to which different loads, e.g. a resistive load or a grid-tied three phase inverter, can be connected. Interleaved converters are used to reduce the switching ripples by shifting the pulse width modulation (PWM) carrier signals by $\frac{2\pi}{n}$, where n is the number of legs. Further advantages are that the setup is easily scalable by adding or removing legs to account for different current requirements. In order to derive a control-oriented model, the following structural assumptions are made: (i) parasitic resistances, inductances and capacities are neglected, (ii) ideal switching and (iii) a purely resistive load are assumed. Assumption (iii) is made since in a generic plug-and-play application the load behavior is unknown, and a purely resistive load can be interpreted as a simple disturbance model for the load (disturbance) current i_{load}. The resulting circuit schematics are presented in Fig. 1, which yields the following equations

$$\begin{aligned}
L_1 \frac{\mathrm{d}i_1}{\mathrm{d}t} &= -(1-s_1)\, v_{\mathrm{B}} + V_{\mathrm{s}}\,, \\
L_2 \frac{\mathrm{d}i_2}{\mathrm{d}t} &= -(1-s_2)\, v_{\mathrm{B}} + V_{\mathrm{s}}\,, \\
L_3 \frac{\mathrm{d}i_3}{\mathrm{d}t} &= -(1-s_3)\, v_{\mathrm{B}} + V_{\mathrm{s}}\,, \\
C_{\mathrm{B}} \frac{\mathrm{d}v_{\mathrm{B}}}{\mathrm{d}t} &= (1-s_1)\, i_1 + (1-s_2)\, i_2 + (1-s_3)\, i_3 - \frac{v_{\mathrm{B}}}{R_0}\,,
\end{aligned}$$

where i_j, v_{B} represent currents and voltage, L_j, C_{B}, R_0 inductances, capacities and resistances, respectively for $j \in \{1,2,3\}$. Switch states are denoted by s_j. The above equations can be simplified with the following assumptions:

- The inductances of the boost legs have the same value $L_1 = L_2 = L_3 =: L_{\mathrm{B}}$.
- Interpreting the physical signals as the sliding average over one PWM period allows to interpret the average of the switching signals $s_{1,2,3}(t)$ as duty cycles $d_{1,2,3}$ [11].
- Since the legs of the interleaved converter are supposed to contribute equally to the supply current, the following is assumed: $i_1 = i_2 = i_3 =: i_{\mathrm{B}}$ and consequently $d_1 = d_2 = d_3 =: d_{\mathrm{B}}$. The internal dynamics not included in the simplified model are stabilized by the indirect, per-leg implementation of the controller.

We obtain the following simplified system

$$\begin{aligned}
L_{\mathrm{B}} \frac{\mathrm{d}\bar{i}_{\mathrm{B}}}{\mathrm{d}t} &= -(1-d_{\mathrm{B}})\, \overline{v}_{\mathrm{B}} + V_{\mathrm{s}}\,, \\
C_{\mathrm{B}} \frac{\mathrm{d}\overline{v}_{\mathrm{B}}}{\mathrm{d}t} &= (1-d_{\mathrm{B}})\, 3\bar{i}_{\mathrm{B}} - \frac{\overline{v}_{\mathrm{B}}}{R_0}\,.
\end{aligned} \tag{1}$$

To obtain a dimension-free representation of (1), cf. [12], we substitute $t = \tau\, t_c$, $\bar{i}_{\mathrm{B}} = \tilde{i}_{\mathrm{B}}\, i_{\mathrm{B,c}}$, $\overline{v}_{\mathrm{B}} = \tilde{v}_{\mathrm{B}}\, v_{\mathrm{B,c}}$, where t_c, $i_{\mathrm{B,c}}$, $v_{\mathrm{B,c}}$ are characteristic values for the dimension-free variables τ, $\tilde{i}_{\mathrm{B}}$, $\tilde{v}_{\mathrm{B}}$. The derivative operator is given by $\frac{\mathrm{d}}{\mathrm{d}t} = \frac{1}{t_c}\frac{\mathrm{d}}{\mathrm{d}\tau}$. Choosing $t_c = \sqrt{L_{\mathrm{B}}\, C_{\mathrm{B}}}$, $i_{\mathrm{B},c} = \sqrt{\frac{C_{\mathrm{B}}}{L_{\mathrm{B}}}}$, $v_{\mathrm{B},c} = V_{\mathrm{s,n}}$, where $V_{\mathrm{s,n}}$ is the nominal supply voltage. This yields the following dimension-free system

$$\begin{aligned}
\frac{\mathrm{d}\tilde{i}_{\mathrm{B}}}{\mathrm{d}\tau} &= -(1-d_{\mathrm{B}})\, \tilde{v}_{\mathrm{B}} + p_1 \\
\frac{\mathrm{d}\tilde{v}_{\mathrm{B}}}{\mathrm{d}\tau} &= (1-d_{\mathrm{B}})\, 3\tilde{i}_{\mathrm{B}} - p_2 \tilde{v}_{\mathrm{B}}\,,
\end{aligned} \tag{2}$$

with the dimension-free parameters $p_1 = \frac{V_{\mathrm{s}}}{V_{\mathrm{s,n}}}$ and $p_2 = \sqrt{\frac{L_{\mathrm{B}}}{C_{\mathrm{B}}}}\frac{1}{R_0}$. By applying the mapping to control notation as given

TABLE I
Mapping to control notation

Name	Physical Notation	Control Notation
States	$\tilde{i}_{\mathrm{B}}$, $\tilde{v}_{\mathrm{B}}$	x_1, x_2
Input	$(1-d_{\mathrm{B}})$	u
Output	$\tilde{v}_{\mathrm{B}}$	y
Parameters	L_{B}, C_{B}	$p_2 = \sqrt{\frac{L_{\mathrm{B}}}{C_{\mathrm{B}}}}\frac{1}{R_0}$
	V_{s}, R_0	$p_1 = \frac{V_{\mathrm{s}}}{V_{\mathrm{s,n}}}$

in Table I, we obtain the following bilinear system

$$\begin{aligned}
\dot{x} &= \begin{bmatrix} 0 & 0 \\ 0 & -p_2 \end{bmatrix} x + \begin{bmatrix} 0 & -1 \\ 3 & 0 \end{bmatrix} x\, \mathrm{sat}_{[0,1]}(u) + \begin{bmatrix} p_1 \\ 0 \end{bmatrix}, \\
y &= \begin{bmatrix} 0 & 1 \end{bmatrix} x\,,
\end{aligned} \tag{3}$$

with $x_1,\, x_2 \in \mathbb{R}_{\geq 0}$. The equilibrium set, valid for $u \in (0,1]$, is parameterized using the setpoint y_d

$$E_{x,u} = \left\{ \left(x_e = \begin{bmatrix} \frac{p_2}{3\,p_1}\, y_d^2 \\ y_d \end{bmatrix}, u_e = \frac{p_1}{y_d} \right) :\, y_d \geq p_1 \right\}. \tag{4}$$

III. Adaptive Control Design for the Interleaved DC/DC Boost converter

As known from literature, the boost converter model is non-minimum phase with respect to the output capacitor voltage as an output. Thus, the direct control of the desired output is not feasible due to the unstable internal dynamics [12]. Consequently, indirect control approaches with the inductor current as an output are preferred, for which the corresponding desired values can be directly obtained from the equilibrium set (4) for a given voltage setpoint. However, the steady-state accuracy will depend on the exact knowledge of the model parameters. The unavoidable uncertainties in real-world

applications are typically compensated by an outer voltage control loop. However, such outer loops can be omitted by leveraging observer based approaches as proposed here.
The design goal is to find an adaptive state feedback control law, such that all trajectories of the closed loop system are bounded and $\lim_{t\to\infty} x(t) = x_e$. Using the I&I framework, cf. [3], allows the separate design of the controller, assuming the knowledge of the system parameters, and the observer system, which together form the observer based adaptive controller, as shown in Fig. 2. The following sections detail the design of the full-information controller and the observer based adaptation.

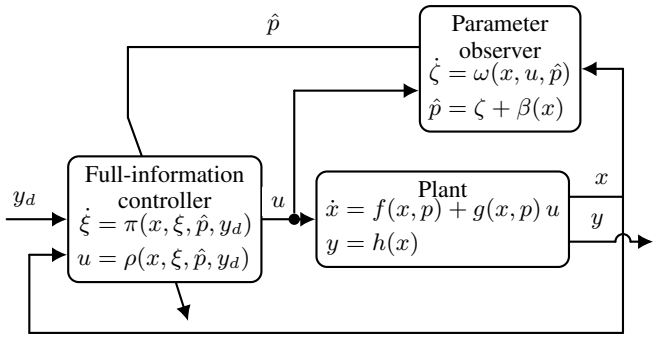

Fig. 2. Signal flowchart of the adaptive control scheme

A. Design of the full-information controller

As a full-information controller, we consider the energy shaping plus damping injection passivity based control (ESDI-PBC), cf. [12], [13] and the references therein. Because adequate tuning of the controller avoids saturation of u, it is omitted during the further course of this paper. In accordance with the I&I framework [3], the controller is designed assuming the knowledge of $p = [p_1 \quad p_2]^\top$, the parameter observer design is described in Sec. III-B. Further, the system is expressed in an energy interpretable form $\mathcal{A}\dot{x} = \mathcal{J}(u)\, x - \mathcal{R}\, x + \mathcal{E}$, where $\mathcal{A}$ is a diagonal positive definite matrix. $\mathcal{J}$ is a skew-symmetric matrix for all u and represents the conservative terms of the system [12]. $\mathcal{R}$ is positive semi-definite and represents the dissipation of the system. Lastly, $\mathcal{E}$ represents the external sources.
For (3) this yields

$$\underbrace{\begin{bmatrix} 1 & 0 \\ 0 & \frac{1}{3} \end{bmatrix}}_{\mathcal{A}} \dot{x} = \underbrace{\begin{bmatrix} 0 & -u \\ u & 0 \end{bmatrix}}_{\mathcal{J}(u)} x - \underbrace{\begin{bmatrix} 0 & 0 \\ 0 & \frac{p_2}{3} \end{bmatrix}}_{\mathcal{R}} x + \underbrace{\begin{bmatrix} p_1 \\ 0 \end{bmatrix}}_{\mathcal{E}} . \tag{5}$$

For the tracking error $e = x - x_e$ with the state reference x_e, the following Lyapunov function candidate is considered

$$V(e) = \frac{1}{2} e^\top \mathcal{A} e \tag{6}$$

Using (5) the derivative of $V(e)$ is given by

$$\dot{V}(e) = e^\top \big((\mathcal{J}(u) - \mathcal{R}) x + \mathcal{E} - \mathcal{A}\dot{x}_e \big) . \tag{7}$$

The following choice

$$\mathcal{A}\dot{x}_e = \mathcal{J}(u) x_e - \mathcal{R} x_e + \mathcal{E} + \mathcal{R}_1\, e\,, \tag{8}$$

yields

$$\dot{V}(e) = -e^\top (\mathcal{R} + \mathcal{R}_1)\, e < 0 \quad \text{for } e \neq 0\,, \tag{9}$$

which holds for $(\mathcal{R} + \mathcal{R}_1)$ positive definite. We choose

$$\mathcal{R}_1 = \begin{bmatrix} R_1 & 0 \\ 0 & 0 \end{bmatrix} . \tag{10}$$

Note that $p_2 > 0$ is ensured for physically meaningful values of L_B, C_B and R_0. From the exogenous system (8), the closed loop control input can be directly derived for the chosen minimum phase output x_1. The remaining equations form the dynamic part of the feedback controller. Assuming a constant reference $x_{1,e}$, and choosing $x_{2,e} = \xi$ in (8) as the state of the controller and using the definition of the tracking error e yields

$$\begin{aligned} u &= \frac{1}{\xi} \big(p_1 + R_1\, (x_1 - x_{1,e}) \big)\,, \\ \dot{\xi} &= 3u\, x_{1,e} - p_2\, \xi\,. \end{aligned} \tag{11}$$

The value for $x_{1,e}$ can be expressed by the desired output y_d using the equilibrium set (4)

$$x_{1,e} = \frac{p_2}{3\, p_1}\, y_d^2\,. \tag{12}$$

We can further leverage the equilibrium set to initialize the state ξ as $\xi_0 = y_d$. The controller given by (11) yields a globally asymptotically stable equilibrium x_e by design.
Remark: As aforementioned, the controller (11) is implemented for each of the legs individually, using the corresponding measurements ($i_{1,2,3}$) to ensure equal leg currents.

B. Design of the I&I parameter observer based adaptation

Now the observer for the model parameters p, which yields the estimates $\hat{p}$, is designed. Thus, we consider the conditions for adaptive I&I stabilizability given in [3]

1) There exists a full-information control law $u = \rho(x, \xi, p)$ such that the closed loop system
$$\dot{x} = f(x, p) + g(x, p)\, \rho(x, \xi, p)\,, \tag{13}$$
has a globally asymptotically stable equilibrium x_e.
2) The continuous mappings $\beta(\cdot)$, $\omega(\cdot)$ exist, such that all trajectories of the extended system
$$\begin{aligned} \dot{\tilde{x}} &= \tilde{f}(\tilde{x}, p) + \tilde{g}(\tilde{x}, p)\, \rho\big(\tilde{x}, \zeta + \beta(\tilde{x})\big)\,, \\ \dot{\zeta} &= \omega(\tilde{x}, \zeta)\,, \end{aligned} \tag{14}$$
with $\tilde{x} = [x \quad \xi]^\top$ and $\hat{p} = \zeta + \beta(\tilde{x})$, are bounded and satisfy
$$\lim_{t\to\infty} \tilde{g}(\tilde{x}, p)\, \rho\big(\tilde{x}, \zeta + \beta(\tilde{x})\big) - \tilde{g}(\tilde{x}, p)\, \rho\big(\tilde{x}, p\big) = 0\,.$$

The first condition is fulfilled by the controller designed in the previous section. Considering the second requirement, we see that the condition is met for all trajectories that are restricted to the manifold [3]

$$\mathcal{M} = \big\{ (\tilde{x}, \hat{p}) \in \mathbb{R}^3 \times \mathbb{R}^2 : \underbrace{\zeta + \beta(\tilde{x})}_{\hat{p}} - p = 0 \big\} . \tag{15}$$

Thus, the aim is to render $\mathcal{M}$ invariant and to ensure that all trajectories converge to $\mathcal{M}$. We introduce the off-the-manifold coordinate $z = \zeta + \beta(\tilde{x}) - p$, with $z = [z_1\ z_2]^\top$ and the continuous mapping $\beta : \mathbb{R}^3 \to \mathbb{R}^2$ with $\beta(\tilde{x}) = [\beta_1(\tilde{x})\ \beta_2(\tilde{x})]$. For the sake of notation we now introduce the linear parameterization of (14)

$$\dot{\tilde{x}} = f_0(\tilde{x})\, p + g_0(\tilde{x})\rho\big(\tilde{x}, \zeta + \beta(\tilde{x})\big)\,. \tag{16}$$

Next, we consider the dynamics of z. Using (16), we obtain

$$\begin{aligned}\dot{z} &= \omega(\tilde{x},\zeta) + \frac{\partial\beta(\tilde{x})}{\partial\tilde{x}}\,\dot{\tilde{x}} + \underbrace{\dot{p}}_{\approx 0} \\ &= \omega(\tilde{x},\zeta) + \frac{\partial\beta(\tilde{x})}{\partial\tilde{x}}\Big(f_0(\tilde{x})\, p + g_0(\tilde{x})\rho\big(\tilde{x}, \zeta + \beta(\tilde{x})\big)\Big)\,,\end{aligned} \tag{17}$$

$\omega(\tilde{x},\zeta)$ is the observer dynamics as introduced in (14).
Remark: assuming $\dot{p} \approx 0$ is a strong assumption, which is in accordance with the modeling assumptions in the present case.
For $\omega(\tilde{x},\zeta)$ we choose

$$\omega(\tilde{x},\zeta) = -\frac{\partial\beta(\tilde{x})}{\partial\tilde{x}}\Big(f_0(\tilde{x})\big(\zeta + \beta(\tilde{x})\big) + g_0\rho\big(\tilde{x}, \zeta + \beta(\tilde{x})\big)\Big). \tag{18}$$

This yields the following for the z-dynamics

$$\dot{z} = -\frac{\partial\beta(\tilde{x})}{\partial\tilde{x}}\Big(f_0(\tilde{x})\, z\Big)\,, \tag{19}$$

from which it is obvious that the choice for $\omega(\tilde{x},\zeta)$ has rendered the manifold $\mathcal{M}$ invariant.
The yet to be determined choice of $\beta(\tilde{x})$ is used to ensure that all trajectories converge to $\mathcal{M}$. For that purpose we consider the following Lyapunov function candidate $V(z) = \frac{1}{2} z^\top z$. Using (17) we obtain the following for the derivative

$$\begin{aligned}\dot{V}(z) = &-z_1^2\frac{\partial\beta_1}{\partial x_1} + z_1 z_2 x_2 \frac{\partial\beta_1}{\partial x_2} + z_1 z_2 \xi \frac{\partial\beta_1}{\partial\xi} \\ &- z_1 z_2 \frac{\partial\beta_2}{\partial x_1} + z_2^2 x_2 \frac{\partial\beta_2}{\partial x_2} + z_2^2 \xi \frac{\partial\beta_2}{\partial\xi}\,.\end{aligned}$$

The negative definiteness of $\dot{V}(z)$ can be ensured with the following choices for $\beta(\tilde{x})$

$$\beta_1 = \alpha_1 \frac{1}{3}\, x_1^3\,, \quad \beta_2 = -\alpha_2 \frac{1}{2}\, x_2^2\,, \tag{20}$$

where $\alpha_1,\ \alpha_2 > 0$ are tunable parameters of the observer.
In summary, we derived the desired mappings $\omega(\tilde{x},\zeta)$ and $\beta(\tilde{x})$ such that the extended system satisfies the requirements, hence our system is I&I stabilizable according to [3].
Using the observer dynamics (18) and the full information control law $u = \rho(\tilde{x}, \hat{p})$ as given in (11), the parameter observer can be expressed as

$$\begin{aligned}\dot{\zeta} &= \begin{bmatrix} -\alpha_1 x_1^2\,(\zeta_1 + \frac{1}{3}\,\alpha_1 x_1^3 - x_2 u) \\ \alpha_2 x_2 (-(\zeta_2 - \frac{1}{2}\alpha_2\, x_2^2)\, x_2 + 3\, x_1 u) \end{bmatrix}\,, \\ \hat{p} &= \zeta + \beta(\tilde{x})\,.\end{aligned} \tag{21}$$

The control law (11) in combination with the parameter observer (21) form the applied adaptive controller.

IV. Experimental analysis of modelling assumption violations

The conducted experiments investigate how violations of the modelling assumptions affect the controller. In the following, the experimental setup is briefly described and the obtained results are presented and discussed.

A. Experimental setup and conducted experiments

The hardware setup is depicted in Fig. 3 and Table II summarizes the parameters. To establish a baseline for the designed controller and to illustrate the influence of the observer tuning parameters, the first experiment (Ex. 1) considers no deliberate model assumption violations. For that purpose a resistive load R_{load} is connected, cf. Fig. 1 with R_{load} as R_0. Next, a realistic application scenario is considered: a PQ-controlled [2], two-level, three phase inverter is connected to the DC-bus as a highly nonlinear load, see Fig. 4. First, no power is injected into the grid and the DC/DC converter only compensates parasitic losses (Ex. 2), violating the load assumption. Next, the nonlinear load is enabled and a step in the desired power is commanded (Ex. 3), thus changing the load type to a different violation of the assumption. Lastly, the supply voltage is changed rapidly while the power setpoint for the load is maintained (Ex. 4), thus violating the load and the slowly changing parameters assumption. Table III summarizes the parameters of the experiments. For better interpretability $\hat{p}_1$, $\hat{p}_2$ are transformed back to their physical meaning, cf. Table I. The initial values for the observed parameters are denoted $\hat{R}_{0,\mathrm{i}}$, $\hat{V}_{\mathrm{s,i}}$ and are chosen deliberately wrong.

TABLE II
Parameters of the hardware and control setup

Name	Value	Description
$L_{\mathrm{B1,2,3}}$	$2.36\,\mathrm{mH}$	Nominal inductivity of the boost legs
C_{B}	$1.6\,\mathrm{mF}$	Nominal capacity of the DC-link
V_{d}	$750\,\mathrm{V}$	Desired DC-bus voltage
f_{s}	$20\,\mathrm{kHz}$	Sampling, control, switching frequency
R_1	20	Control parameter
α_1	$5 \cdot 10^3$	Observer tuning parameter
α_2	$45 \cdot 10^{-3}$	Observer tuning parameter

TABLE III
Parameters of the experiments

Exp.	$\hat{R}_{0,i}$	$\hat{V}_{\mathrm{s,i}}$	P_{load}	R_{load}	V_{s}
Ex. 1	$60\,\Omega$	$600\,\mathrm{V}$	n.a.	$200\,\Omega$	$550\,\mathrm{V}$
Ex. 2	$60\,\Omega$	$600\,\mathrm{V}$	$0\,\mathrm{W}$	n.a.	$550\,\mathrm{V}$
Ex. 3	n.a.	n.a.	$0 \to 5\,\mathrm{kW}$	n.a.	$550\,\mathrm{V}$
Ex. 4	n.a.	n.a.	$5\,\mathrm{kW}$	n.a.	$600 \to 500\,\mathrm{V}$

B. Experimental results and discussion

1) Ex. 1 - Resistive load and observer tuning: Fig. 5 and 6, show the influence of the observer tuning parameters α_1, α_2, the trade-off between rate of convergence and noise amplification can be observed in both cases. The following experiments

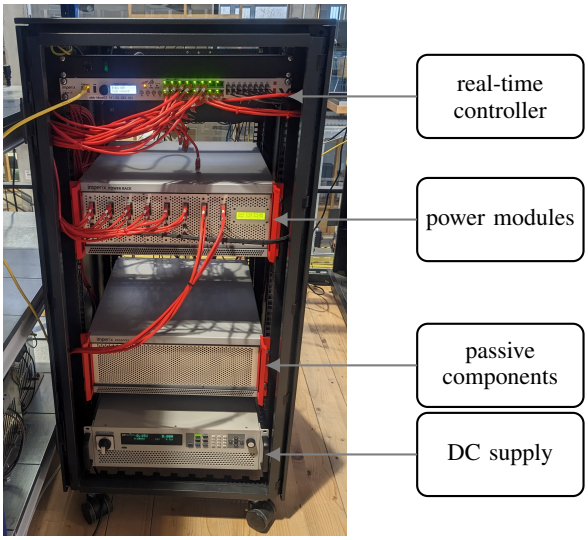

Fig. 3. Image of the hardware setup used for the presented experiments

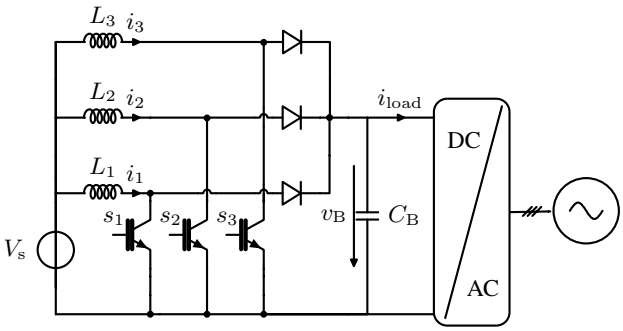

Fig. 4. Circuit diagram of the experimental setup.

are conducted with the values given in Table II. Measurements for the DC quantities of Ex. 1 are shown in Fig. 7. At $t = 0$, the controller is enabled and the control goal of regulating v_{B} is achieved. The observed supply voltage converges within roughly 20 ms. In steady state the value of $\hat{V}_{\text{s}}$ is around 2 % smaller than the nominal value. This is expected behavior, since the observer model does not contain parasitic losses, e.g. resistance of L_{B}, and thus interprets them as a reduced supply voltage. Fig. 8 shows the leg currents and results shows that the assumption $i_1 = i_2 = i_3 =: i_{\text{B}}$ holds. Fig. 6 shows the

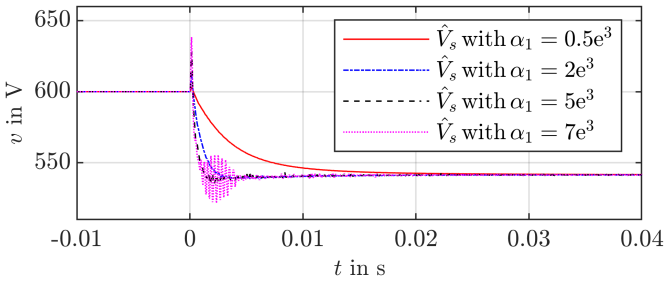

Fig. 5. Tuning of α_1 using the experimental setup of Ex. 1.

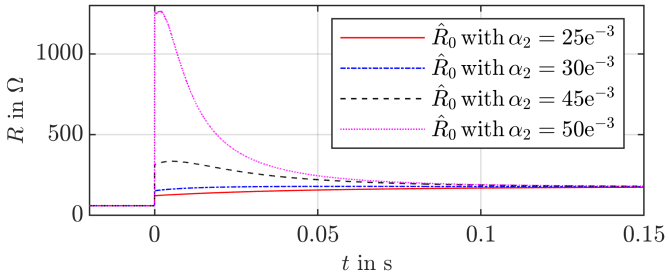

Fig. 6. Tuning of α_2 using the experimental setup of Ex. 1.

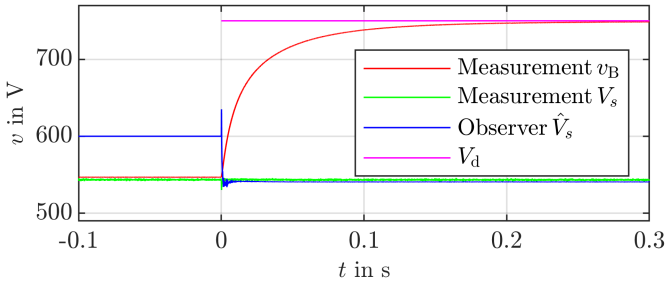

Fig. 7. Measurements and observations of the DC quantities during Ex. 1.

observed load resistance $\hat{R}_0$. In steady state the value differs roughly 11.5% from the nominal value. This is acceptable considering common uncertainties for passive electrical components as well as parasitic losses of the capacitor and switches which are interpreted as additional load.

2) Ex. 2 - Parasitic losses only: For Ex. 2 no load is connected, thus only parasitic losses need to be compensated. At $t = 0\,\text{s}$ the controller is enabled, Fig. 9 shows the observer results. Again, the supply voltage estimate $\hat{V}_{\text{s}}$ converges quickly and shows an offset of around 2 %. The value for $\hat{R}_0$ converges to roughly 3200 Ω and exhibits significant noise. This can be explained by large contribution of the measurement noise to the small leg currents. Note that the parallel connection of the observed losses $\hat{R}_0 = 3200\,\Omega$ and $R_{\text{load}} = 200\,\Omega$ roughly yields the value for $\hat{R}_0$ in Ex. 1.

3) Ex. 3 - Nonlinear load: In Ex. 3 the behavior of the adaptive control scheme during a load step of the nonlinear load at $t = 0\,\text{s}$ is studied. Fig. 10 shows the DC quantities, v_{B} returns to the desired value after 0.12 s. The increase of the leg currents due to the load step leads to larger resistive losses,

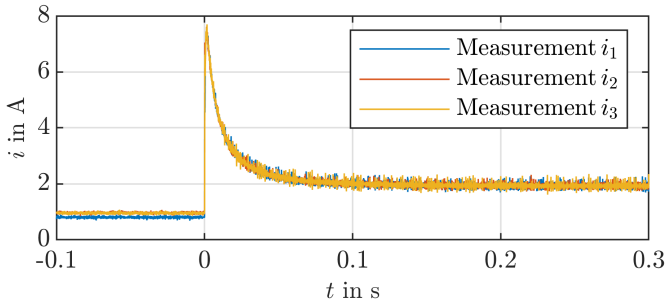

Fig. 8. Leg currents of the interleaved boost converter during Ex. 1.

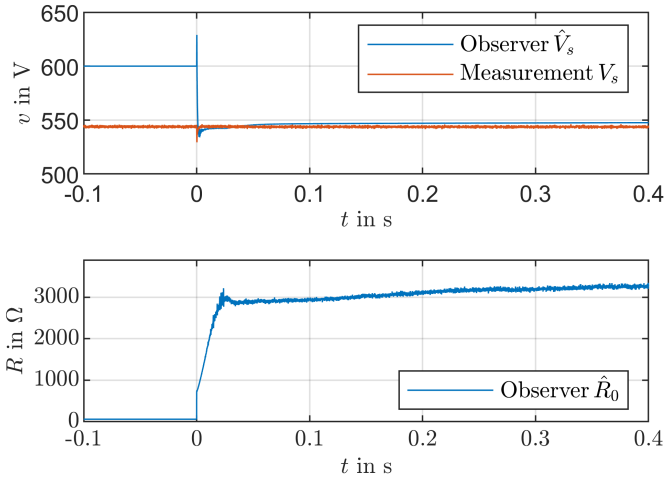

Fig. 9. Observed parameters during Ex. 2.

which manifests in the reduction of $\hat{V}_\mathrm{s}$. Fig. 11 shows the

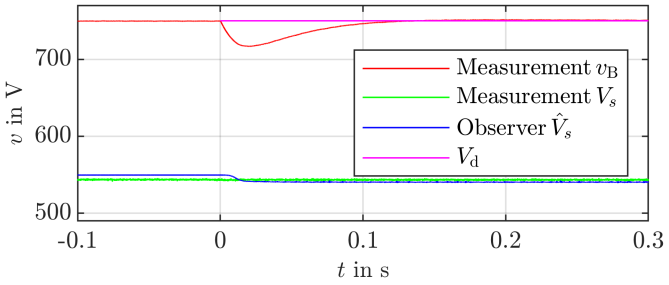

Fig. 10. Measurements and observations of the DC quantities during Ex. 3.

observed load resistance, the value converges after $t = 0.05\,\mathrm{s}$ to the new steady state. It can be noted that for larger loads the noise in the observation vanishes, due to the better signal to noise ratio.

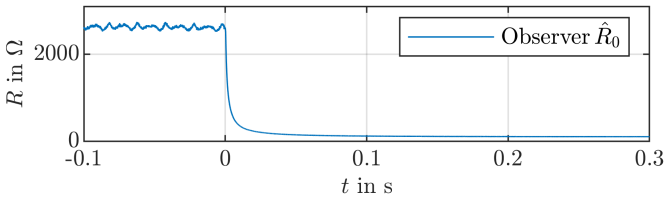

Fig. 11. Observed load resistance during Ex. 3.

4) Ex. 4 - Sudden supply voltage change: At $t = 0\,\mathrm{s}$, V_s suddenly drops, while the nonlinear load maintains the power setpoint. Fig. 12 shows that $\hat{V}_\mathrm{s}$ closely follows the measured voltage during the rapid change and v_B returns to the desired value after $0.07\,\mathrm{s}$.

V. Conclusion

The present paper illustrates the design of an observer based adaptive controller for an interleaved DC/DC boost converter, using the I&I framework with strong modelling assumptions and simplifications. The experimental results show that the

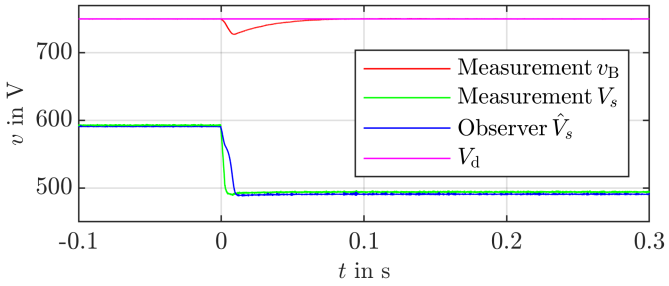

Fig. 12. Measurements and observations of the DC quantities during Ex. 4.

combination of observer design for the plant and per-leg implementation of the controller is suitable. Despite the simplifications, the approach is able to accommodate parametric and ambient uncertainties of the plant and achieves the control objective of voltage regulation. This even holds for the violation of several modelling assumptions, such as a nonlinear, constant power load instead of a purely resistive load, or quickly changing parameters instead of constant values. Further, the obtained values for the observed parameters show the expected behavior and remain physically interpretable for all conducted experiments.

References

[1] A. Sajadi, R. W. Kenyon, and B.-M. Hodge, "Synchronization in electric power networks with inherent heterogeneity up to 100% inverter-based renewable generation," *Nature Communications*, vol. 13, no. 1, May 2022.

[2] J. Rocabert, A. Luna, F. Blaabjerg, and P. Rodríguez, "Control of power converters in AC microgrids," *IEEE Transactions on Power Electronics*, vol. 27, no. 11, pp. 4734–4749, Nov. 2012.

[3] A. Astolfi, D. Karagiannis, and R. Ortega, *Nonlinear and Adaptive Control with Applications*. London: Springer, 2008.

[4] M. Malekzadeh, A. Khosravi, and M. Tavan, "An immersion and invariance based input voltage and resistive load observer for DC–DC boost converter," *SN Applied Sciences*, vol. 2, no. 1, Dec. 2019.

[5] ——, "A novel adaptive output feedback control for DC–DC boost converter using immersion and invariance observer," *Evolving Systems*, vol. 11, no. 4, pp. 707–715, Jan. 2019.

[6] W. He, C. A. Soriano-Rangel, R. Ortega, A. Astolfi, F. Mancilla-David, and S. Li, "Energy shaping control for buck–boost converters with unknown constant power load," *Control Engineering Practice*, vol. 74, pp. 33–43, May 2018.

[7] W. He and R. Ortega, "Design and implementation of adaptive energy shaping control for DC–DC converters with constant power loads," *IEEE Transactions on Industrial Informatics*, vol. 16, no. 8, pp. 5053–5064, Aug. 2020.

[8] W. He, M. M. Namazi, H. R. Koofigar, M. A. Amirian, and F. Blaabjerg, "Stabilization of DC–DC buck converter with unknown constant power load via passivity-based control plus proportion-integration," *IET Power Electronics*, vol. 14, no. 16, pp. 2597–2609, Nov. 2021.

[9] C. A. Soriano-Rangel, W. He, F. Mancilla-David, and R. Ortega, "Voltage regulation in buck–boost converters feeding an unknown constant power load: An adaptive passivity-based control," *IEEE Transactions on Control Systems Technology*, vol. 29, no. 1, pp. 395–402, Jan. 2021.

[10] L. Xu, R. Ma, R. Xie, J. Xu, Y. Huangfu, and F. Gao, "Open-circuit switch fault diagnosis and fault- tolerant control for output-series interleaved boost DC–DC converter," *IEEE Transactions on Transportation Electrification*, vol. 7, no. 4, pp. 2054–2066, Dec. 2021.

[11] R. W. Erickson and D. Maksimović, *Fundamentals of Power Electronics*, 3rd ed. Cham: Springer, 2020.

[12] H. J. Sira-Ramirez and R. Silva-Ortigoza, *Control Design Techniques in Power Electronics Devices*. London: Springer, Sep. 2006.

[13] R. Ortega, A. Loría, P. J. Nicklasson, and H. Sira-Ramirez, *Passivity-based Control of Euler-Lagrange Systems*. London: Springer, 1998.